

# Quad-HIDAC PET: Comparison of Four Image Reconstruction Techniques for High Resolution Imaging

Richard J. Walledge, Roido Manavaki, Andrew J. Reader, Alan P. Jeavons,  
Peter J. Julyan, Sha Zhao, David L. Hastings and Jamal Zweit

**Abstract--** The quad-HIDAC PET scanner offers unparalleled high resolution PET imaging capability (<1 mm), combined with notable count rate performance (400 kcps) and sensitivity (up to 2% with scatter correction). To some extent the image resolution realized by the system is determined by the choice of image reconstruction algorithm. This work compares 4 reconstruction techniques applied to data from the quad-HIDAC scanner: 2 iterative methods (ROPLE and 3D OSEM) and 2 analytic methods (BPF and 3D RP). These four methods were chosen so as to include both a list-mode based and a projection-based method in each category. The algorithms were compared in terms of contrast, noise and resolution for a specially designed cylindrical phantom. The results indicate that the iterative methods offer improved resolution and contrast for a given noise level compared to the analytic methods. Of these iterative methods, the new list-mode technique (ROPLE) performed better than the projection-based technique.

## I. INTRODUCTION

SMALL animal imaging opens new possibilities for biomedical research, offering the ability to assess new targeted treatments whilst still in early development and allowing animal models of human disease to be analyzed. This research has called for higher resolution Positron Emission Tomography (PET) scanners, which in turn demand image reconstruction techniques which are able to make full use of the available scanner resolution. For the quad-HIDAC scanner [1], which has approximately  $10^{12}$  lines of response (LORs), any use of projection data in the reconstruction may compromise the system's spatial sampling capability (storage of all possible projection elements is not only unfeasible, but also yields an exorbitant reconstruction time). To assess the significance of this, two projection data techniques: 3D Reprojection (3DRP) [2] and 3D Ordered Subsets

Expectation-Maximization (OSEM) [3], have been compared with two list-mode techniques: Backproject then Filter (BPF) [4] and the new Regularized One-Pass List-mode EM (ROPLE) algorithm [5], an enhanced version of the Fast Accurate Iterative Reconstruction (FAIR) algorithm [6]. Apart from storage requirements, choice of reconstruction algorithm is also influenced by the processing time. Iterative methods by definition tend to require more time, while analytic methods are in general quicker for the same size array.

## II. THEORY

### A. Projection Data Methods (3D RP & 3D OSEM)

The 3D RP has often been regarded as the gold standard analytic reconstruction algorithm for 3D PET. Initially, the completely measured projections are processed with 2D Filtered Backprojection (FBP), to produce a low-statistics first estimate of the image. This volume is then forward-projected to fill in the missing projections.

3D OSEM is an iterative approach, based on Expectation Maximization-Maximum Likelihood (EM-ML) and using azimuthal subsets of the projection data to accelerate convergence. If the probability of an emission from voxel  $j$  being detected along line of response (LOR)  $i$  is  $a_{ij}$ , using measured data  $m$ , for a given subset  $S_i$ , the update equation for the value  $n$  at update  $k$  is:

$$n_j^{k,l+1} = \frac{n_j^{k,l}}{\sum_{i \in S_i} a_{ij}} \sum_{i \in S_i} a_{ij} \frac{m_i}{q_i^{k,l}} \quad (1)$$

where

$$q_i^k = \sum_{j=1}^J a_{ij} n_j^k \quad (2)$$

is the expected count in LOR  $i$  if the intensity was  $n$ .

---

Manuscript received November 9, 2001.

R. J. Walledge, R. Manavaki, A. J. Reader and J. Zweit are with the Department of Instrumentation and Analytical Science (DIAS), at UMIST, Manchester, PO BOX 88, M60 1QD, UK (telephone: (44)-161-200-4880, e-mail: richard.walledge@stud.umist.ac.uk).

A. P. Jeavons is the director of Oxford Positron Systems, Oxford, UK.

S. Zhao, P. J. Julyan, D. L. Hastings and J. Zweit are with the Paterson Institute of Cancer Research and Christie Hospital NHS Trust, Manchester, UK

### B. List-mode Methods (BPF & ROPLE)

The backproject then filter method attempts to obtain the image  $f(r)$  by using a backprojected image  $g(r)$  and the point response function  $h(r)$  of the system. The filtering step is a frequency domain multiplication. Taking Fourier transforms:

$$f(\mathbf{k}) = FT^{-1}(G(\mathbf{k}) / H(\mathbf{k})) \quad (3)$$

The ROPLE algorithm is based on the pure form of the list-mode EM-ML algorithm, given by:

$$n_j^{k+1} = \frac{n_j^k}{\sum_{i=1}^M a_{ij}} \sum_{i=1}^M a_{ij} \frac{1}{q_i^k} \quad (4)$$

where the measured list-mode data are now implicitly 1 for each acquired LOR. The algorithm can be extended to incorporate subsets:

$$n_j^{k+1} = \frac{n_j^k}{\sum_{i \in s} a_{ij}} \sum_{i \in s} a_{ij} \frac{1}{q_i^k} \quad (5)$$

where only a subset  $s$  of the  $M$  total LORs is used in each update. Each subset  $s$  ( $s=1 \dots S$ ) consists of an equal number of list-mode events. It is well known that this algorithm, just as with the normal projection data based EM-ML, can lead to noisy reconstructions. In this work, the median root prior[7] was used to regularize the reconstruction. In addition, both OSEM and ROPLE incorporated resolution recovery via a spatially extensive system model[5].

## III. METHODS

### A. Line Source

A 0.5 mm diameter aluminum wire (length ~100 mm) was irradiated with  $^{22}\text{Na}$ , giving about 1 MBq of activity. This line source was placed along the axis of a 16-module quad-HIDAC and scanned for 20 minutes, acquiring 10.8 million events. Four different reconstruction techniques were applied to the data, using an array  $64 \times 64 \times 512$ , and voxels of 0.2 mm. For the projection-based methods, 60  $\phi$  samples ( $3^\circ$  interval) were used, with 31  $\theta$  samples ( $3^\circ$  interval). For 3D RP and BPF, different cut-off frequencies in the range 0.5 to 1.0 were used for frequency domain windowing. For OSEM and ROPLE, the median root prior was used for regularization, with varying strengths in the range 0.1 to 0.9. Profiles were taken through the line in the radial and tangential directions, and these were interpolated to 10 times their original length. The full-width half max (FWHM) and full-width tenth max (FWTM) were taken along each line profile, and these values were averaged over the axial length of the source.

### B. Cylindrical Phantom

A cylindrical phantom (30 mm internal diameter, 50 mm internal length) containing 4 cylindrical inserts (10 mm

diameter, 20 mm length) was filled with FDG of activity 2.13, 0.94, 0.39 and 0.29 MBq, and a background of 0.12 MBq. This phantom was scanned with the quad-HIDAC for one hour. 106 million list-mode events were acquired, and the four reconstruction techniques were applied to the data. For the projection-based methods, a set of projections was used with  $128 \times 128$  bins (0.5 mm sampling in both  $y'$  and  $z'$  directions), 96  $\phi$  samples ( $1.9^\circ$  interval) and 27  $\theta$  samples ( $3.5^\circ$  interval). All reconstructions used 0.5 mm voxels in a  $128^3$  image array.

The following figures of merit (FOMs) were evaluated for the reconstructed phantom images: contrast, noise and axial uniformity. Contrast was measured by taking a region from within each of the four inserts, and then expressing the contrast for cylinder  $i$  as

$$C_i = \frac{\text{mean}_i}{\text{mean}_{\text{hottest}}} \bigg/ \frac{\text{true}_i}{\text{true}_{\text{hottest}}} \quad (6)$$

Noise was measured using the standard deviation of voxel values in the inserts (expressed as a fraction of the mean for that insert). This gave a contrast measure for 3 different activity levels, and noise measure for 4 activity levels.

### C. Rat Bone Scan

A 500g rat was injected with 17 MBq of F- activity, and scanned with the quad-HIDAC, with 145 million list-mode events being acquired in 30 minutes. The four algorithms were used to reconstruct the data into a  $128 \times 128 \times 512$  array, with 0.5 mm voxels. 3DRP and OSEM used parallel projections with 96  $\phi$  samples ( $1.9^\circ$  interval) and 25  $\theta$  samples ( $4^\circ$  interval). The reconstructions were compared visually.

## IV. EXPERIMENTAL RESULTS

Figure 1 shows the reconstruction times for a number of image sizes, using a typical Pentium III class workstation (700MHz, 768 MB RAM).

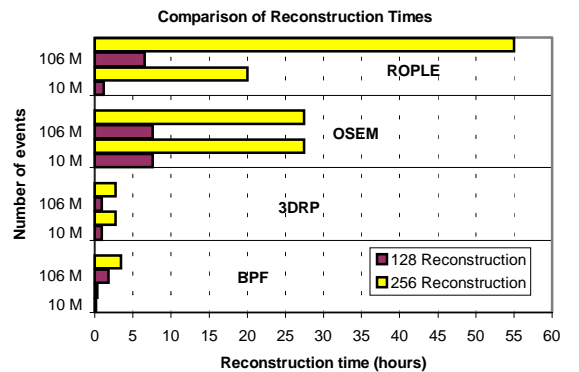


Fig. 1. Comparison of reconstruction time in minutes for the four algorithms, for two data set sizes (106 million and 3 million events). Two image sizes ( $128^3$  and  $256^3$  voxels) are shown. The times for OSEM and 3D RP do not include rebinning into projections. The times for OSEM and ROPLE are for one iteration of 50 subsets.

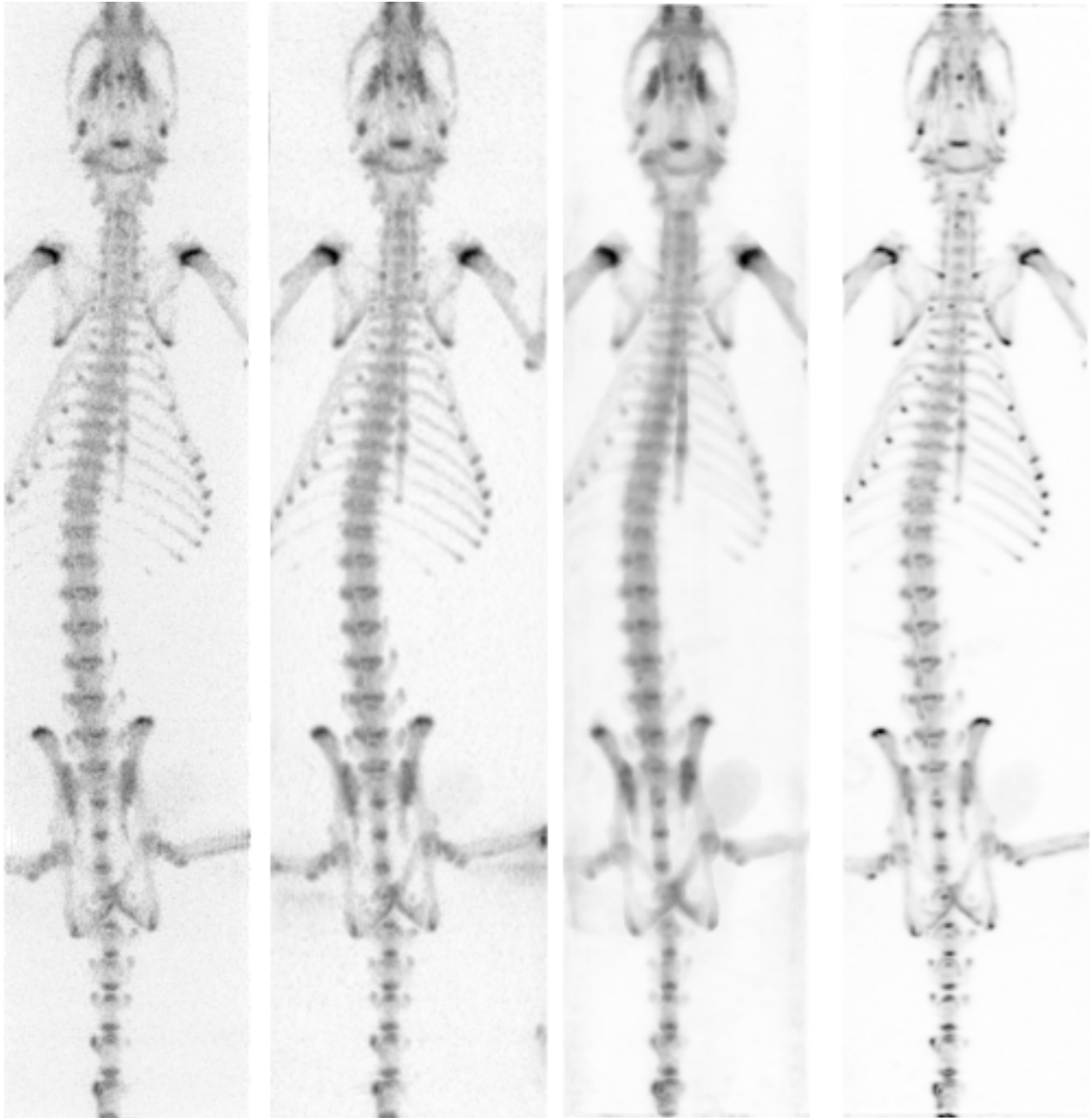


Fig. 2. Visual comparison of reconstructions of an  $^{18}\text{F}$  rat scan. Shown is a pair of maximum intensity coronal projections for (left to right) BPF, 3DRP, OSEM and ROPLC. Each image is from an array of  $128 \times 128 \times 512$  voxels (size 0.5 mm). In all cases, detail in the spine and vertebrae is visible, and with the iterative methods there is a clear difference in background noise compared to the analytic methods. The scan was with 17 MBq of activity, and consisted of 145 million events acquired in 30 minutes.

Slices from images of the rat bone scan are shown in Figure 2.

Figure 3 shows the range of the FWHM resolution of the reconstructed line source, coupled with the noise values for the hottest cylinder.

Figure 4 shows the range of the FWTM resolution of the reconstructed line source, coupled with the noise values for the coldest cylinder.

Figure 5 shows the contrast for the four algorithms.

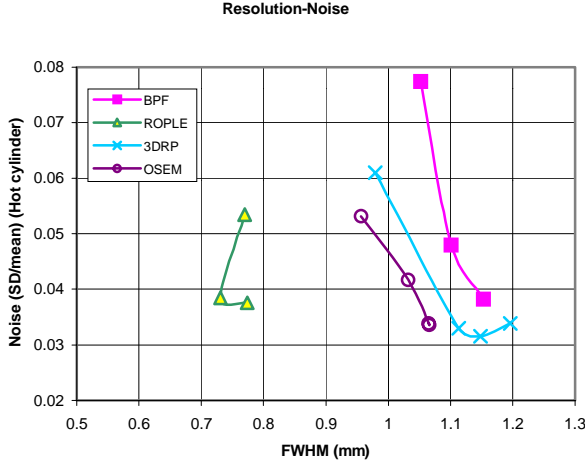


Fig. 3. Tradeoff curves for the resolution (FWHM) against noise for the four algorithms. Noise is measured as the SD of voxel values in the hottest cylindrical insert (2.13 MBq), over the mean value. For 3D RP and BPF, different cut-off frequencies were used for frequency domain windowing. For OSEM and ROPL, different values for the strength of the median root prior were used.

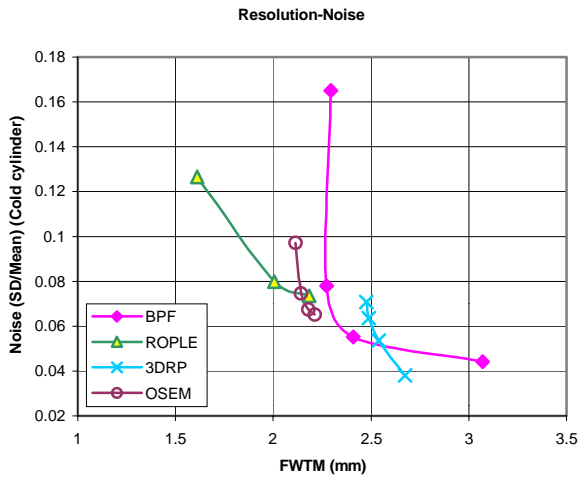


Fig. 4. Tradeoff curves for the resolution (FWTM) against noise for the four algorithms. Noise is measured as the SD of voxel values in the coldest cylindrical insert (0.29 MBq), over the mean value. For 3D RP and BPF, different cut-off frequencies were used for frequency domain windowing. For OSEM and ROPL, different values for the strength of the median root prior were used.

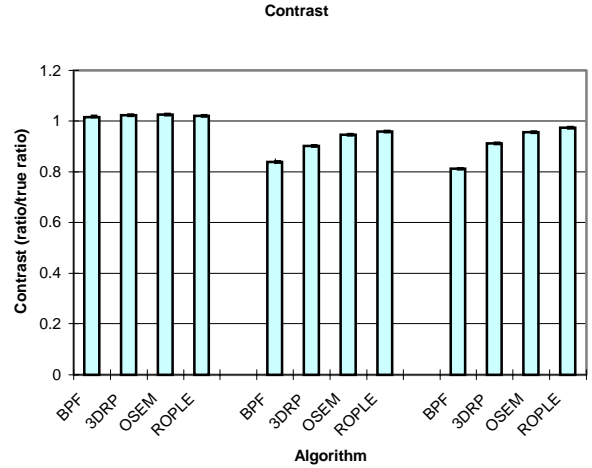


Fig. 5. Contrast values for the four algorithms. The three groups represent the second, third and fourth inserts. Contrast was calculated as the mean count in a cylinder of interest as a ratio of the mean of the hottest cylinder, then this ratio was expressed as a fraction of the known true values. The main bars represent the actual contrast values, with the error-bars representing the maxima and minima (obtained by using different reconstruction parameters)

## V. DISCUSSION

### A. Processing Times

For high-statistics imaging, the list-mode based methods suffer an increase in processing time due to a larger number of events. Conversely, this also means that in low-statistics situations such as dynamic scans, they operate more quickly than the projection-based methods. However, list-mode methods have the property that increasing the matrix size by a factor of  $2^3$  does not lead to a factor of 8 increase in the reconstruction time. As memory limitations become less of an issue and so matrix sizes increase, this gain becomes more important.

### B. Resolution- Noise Tradeoff

In terms of FWHM resolution, there is a marked difference between the iterative and analytic approaches. As can be seen in Figure 3, the two analytic methods, BPF and 3D RP, offer comparable resolution, although 3D RP has wider range of values at both ends of the resolution scale. OSEM has superior resolution values compared to the analytic methods, while ROPL consistently achieves the highest resolution of all ( $\beta = 0.5$  gives a mean FWHM value of 0.73 mm). However, these two methods also suffer a higher noise level compared to 3D RP. With a Colsher filter, the noise values for the hottest insert with 3DRP are quite consistent and are the lowest of all the algorithms tested here. It is only with a ramp filter that the values rise considerably.

Trends for the FWTM resolution are similar to those for FWHM, with the exception that there are some crossovers between the curves. Although ROPL was still the best, the difference in resolution was not so clear-cut. 3DRP suffered

slightly more than the other algorithms for FWTM, although its noise properties were still the best.

### C. Contrast

The contrast results for all methods were comparable, showing only minor differences. 3DRP and OSEM were the highest for the high activity level (0.94 MBq). The fact that some of the final values are above 100% can be explained either by the target cylinder being over-represented, or by the hottest cylinder being under-represented.

ROPLE offered slightly better performance for the low activity levels (0.39 and 0.29 MBq), whereas BPF was generally slightly inferior to all the other methods. The contrast difference between the list-mode and the projection-based methods was not readily observable: in some cases the two projection-based methods appear inside the range for the two list-mode techniques. For three of the four techniques considered here, varying the smoothing and regularization had virtually no significant effect on the contrast levels.

## VI. CONCLUSION

Iterative image reconstruction offers improved resolution and contrast at a given noise level when compared to analytic methods. Based on the FOMs studied in this work, ROPLE is the best all-round reconstruction algorithm for use with quad-HIDAC data.

Only one disadvantage of this technique was apparent: that of the long processing times required. Acceleration would be possible by reducing the number of redundant calculations that are performed.

Further work for this study will be to incorporate full data correction techniques into these algorithms, to allow for effects such as scatter, and random events.

There is also the possibility of testing these algorithms for dynamic PET imaging with the quad-HIDAC, where the high sensitivity of this scanner will allow for a data acquisition to be broken down into data sets of shorter duration.

## VII. ACKNOWLEDGMENT

The authors gratefully acknowledge Drs Missimer, Honer, Ametamey and Prof Schubiger (Paul Scherrer Institute) for supplying the raw list-mode data for the rat scans.

## VIII. REFERENCES

- [1] A. P. Jeavons, R. A. Chandler, C. A. R. Dettmar, "A 3D HIDAC-PET Camera with Sub-millimetre Resolution for Imaging Small Animals", *IEEE Trans Nuc Sci*, vol 46, pp 468-478, 1999.
- [2] P. E. Kinahan and J. G. Rogers, "Analytic three-dimensional image reconstruction using all detected events", *IEEE Trans. Nucl. Sci.*, vol 36, pp 964-968, 1989.
- [3] H. M. Hudson and R. S. Larkin, "Accelerated Image Reconstruction Using Ordered Subsets of Projection Data", *IEEE Trans. Med. Im.*, vol 13, pp 601-609, 1994.
- [4] G. Chu and K. C. Tam, "Three-dimensional imaging in the positron camera using Fourier techniques", *Phys. Med. Biol.*, vol 2, pp 245-265, 1977.
- [5] A. J. Reader, S. Ally, F. Bakatselos, R. Manavaki, R. J. Walledge, A. P. Jeavons, P. J. Julyan, S. Zhao, D. L. Hastings and J. Zweit "Regularized One-Pass List-Mode EM Algorithm for High Resolution 3D PET Image Reconstruction into Large Arrays" *IEEE NSS-MIC Conference Record*, San Diego, CA, Nov 2001.
- [6] A. J. Reader, K. Erlandsson, M. A. Flower and R. J. Ott, "Fast Accurate Iterative Reconstruction for Low-Statistics Positron Volume Imaging", *Phys. Med. Biol.*, vol. 43, pp.835-846, 1998.
- [7] S. Alenius and U. Ruotsalainen, "Bayesian image reconstruction for emission tomography based on median root prior", *Eur Jour of Nuc Med*, vol 24, pp258-265, 1997.